J|A|C|S
ARTICLES
Published on Web 10/19/2004

Synthesis, Self-Assembly, and Characterization of Supramolecular Polymers from Electroactive Dendron Rodcoil Molecules

Benjamin W. Messmore, James F. Hulvat, Eli D. Sone, and Samuel I. Stupp*

Contribution from the Department of Chemistry, the Department of Materials Science & Engineering, and the Feinberg School of Medicine, Northwestern University, Evanston, Illinois 60208

Received February 6, 2004; E-mail: s-stupp@northwestern.edu

Abstract: We report here the synthesis and self-assembly of a series of three molecules with dendron rodcoil architecture that contain conjugated segments of oligo(thiophene), oligo(phenylene-vinylene), and oligo(phenylene). Despite their structural differences, all three molecules yield similar self-assembled structures. Electron and atomic force microscopy reveals the self-assembly of the molecules into high aspect ratio ribbon-like nanostructures which at low concentrations induce gelation in nonpolar solvent. Self-assembly results in a blue-shifted absorption spectrum and a red-shifted, quenched fluorescence spectrum, indicating aggregation of the conjugated segments within the ribbon-like structures. The assembly of these molecules into one-dimensional nanostructures is a route to $\pi-\pi$ stacked supramolecular polymers for organic electronic functions. In the oligo(thiophene) derivative, self-assembly leads to a 3 orders of magnitude increase in the conductivity of iodine-doped films due to self-assembly. We also found that electric field alignment of these supramolecular assemblies can be used to create arrays of self-assembled nanowires on a device substrate.

Introduction

Electronically active organic molecules are of great interest for electronic devices because of low processing costs and desirable mechanical properties as compared to their inorganic counterparts.[1−3] Conductive polymers have desirable mechanical properties, but often lack long-range molecular order due to defects arising during polymerization, thus lowering device performance.[4] Molecular order can be achieved through vapor deposition of small oligomers, resulting in crystalline films, but with higher processing costs.[5] The recent strategies of self-assembly and supramolecular chemistry are interesting alternatives for the bottom-up design of organic electronic devices.[6−12]

Our group reported recently on a family of self-assembling triblock molecules with generation one 3,5 dihydroxy-benzoic ester dendritic segments, rigid rod-like segments, and various flexible coil-like segments, referred to as dendron rodcoil (DRC) molecules.[13−15] In certain solvents and at low weight percentages, DRC molecules form self-supporting gels that result from a 3-D network of high aspect ratio, ribbon-like nanostructures. Due to their unique triblock architecture, DRC molecules aggregate into one-dimensional nanostructures through specific and nonspecific interactions. Hydrogen bonding between dendrons and $\pi-\pi$ stacking between rods enable assembly in one dimension, while the conformationally flexible coil solubilizes the nanostructure and frustrates further crystallization. The ribbons are ~10 nm wide, 1.5 nm thick, and micrometers long. Head-to-head packing of the hydrogen-bonded dendrons has been inferred from X-ray crystallography of a model compound.[13]

In this work, we have designed and synthesized DRC molecules containing phenyl-quater(thiophene), ter(phenylene vinylene), and quater(phenylene) segments as part of the rod segment of the DRC structure. We have characterized the self-assembling behavior and electronic properties in those containing phenyl quater(thiophene) segments.

Results and Discussion

Synthesis. The synthesis of the dendron-biphenyl segment (**14**) is based on orthogonal protection/deprotection chemistry

(1) Katz, H. E.; Bao, Z. N.; Gilat, S. L. *Acc. Chem. Res.* **2001**, *34*, 359−369.
(2) Dimitrakopoulos, C. D.; Mascaro, D. J. *IBM J. Res. Dev.* **2001**, *45*, 11−27.
(3) Martin, R. E.; Diederich, F. *Angew. Chem., Int. Ed.* **1999**, *38*, 1350−1377.
(4) Bao, Z. N.; Rogers, J. A.; Katz, H. E. *J. Mater. Chem.* **1999**, *9*, 1895−1904.
(5) Garnier, F.; Yassar, A.; Hajlaoui, R.; Horowitz, G.; Deloffre, F.; Servet, B.; Ries, S.; Alnot, P. *J. Am. Chem. Soc.* **1993**, *115*, 8716−8721.
(6) Lehn, J. M. *Supramolecular Chemistry*; VCH Press: New York, 1995.
(7) Stupp, S. I.; LeBonheur, V.; Walker, K.; Li, L. S.; Huggins, K. E.; Keser, M.; Amstutz, A. *Science* **1997**, *276*, 384−389.
(8) Hulvat, J. F.; Stupp, S. I. *Angew. Chem., Int. Ed.* **2003**, *42*, 778−781.
(9) Yoshio, M.; Mukai, T.; Ohno, H.; Kato, T. *J. Am. Chem. Soc.* **2004**, *126*, 994−995.
(10) Schenning, A.; Kilbinger, A. F. M.; Biscarini, F.; Cavallini, M.; Cooper, H. J.; Derrick, P. J.; Feast, W. J.; Lazzaroni, R.; Leclere, P.; McDonell, L. A.; Meijer, E. W.; Meskers, S. C. J. *J. Am. Chem. Soc.* **2002**, *124*, 1269−1275.
(11) Hill, J. P.; Jin, W.; Kosaka, A.; Fukushima, T.; Ichihara, H.; Shimomura, T.; Ito, K.; Hashizume, T.; Ishii, N.; Aida, T. *Science* **2004**, *304*, 1481−1483.
(12) Samori, P.; Francke, V.; Mullen, K.; Rabe, J. P. *Chem.-Eur. J.* **1999**, *5*, 2312−2317.
(13) Zubarev, E. R.; Pralle, M. U.; Sone, E. D.; Stupp, S. I. *J. Am. Chem. Soc.* **2001**, *123*, 4105−4106.
(14) Zubarev, E. R.; Pralle, M. U.; Sone, E. D.; Stupp, S. I. *Adv. Mater.* **2002**, *14*, 198−203.
(15) Lecommandoux, S.; Klok, H. A.; Sayar, M.; Stupp, S. I. *J. Polym. Sci., Part A* **2003**, *41*, 3501−3518.

10.1021/ja049325w CCC: $27.50 **© 2004 American Chemical Society**

Scheme 1. Chemical Structures of DRCs

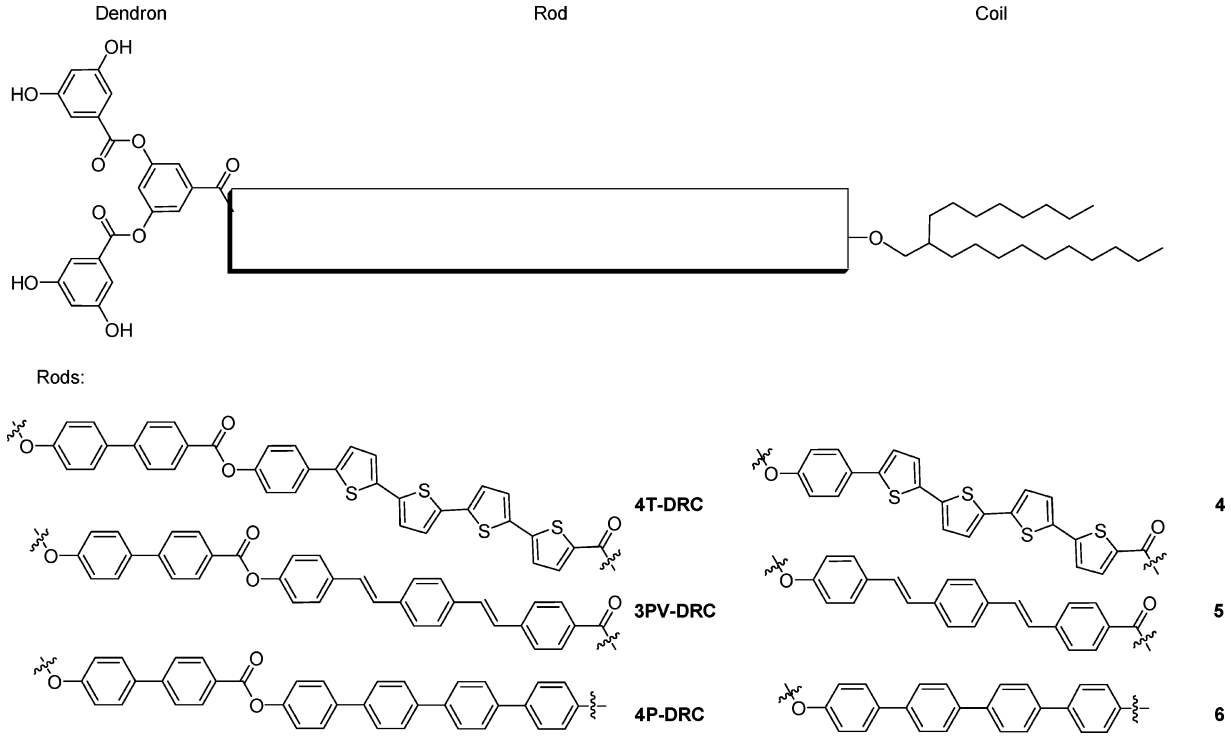

Scheme 2. Synthesis of Dendron[a]

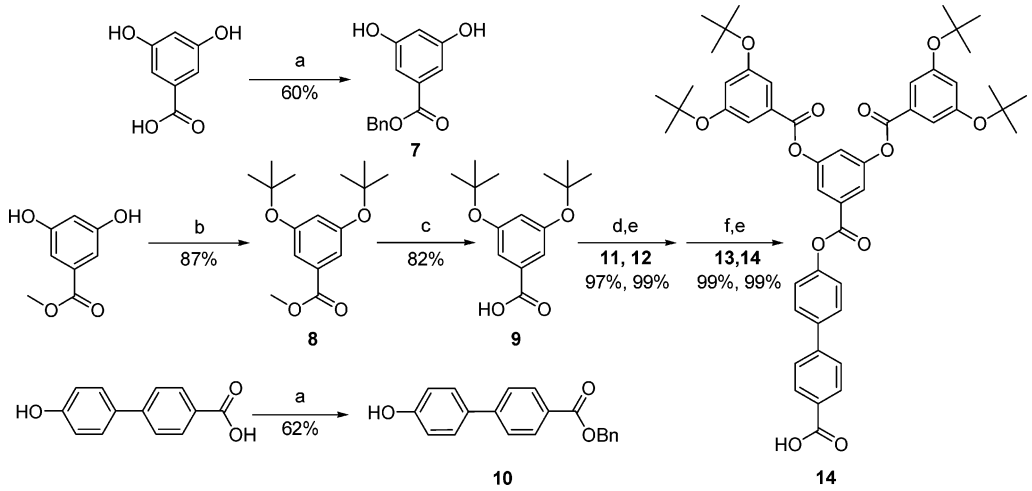

[a] (a) BnCl, K_2CO_3, DMF, room temperature; (b) isobutylene, H_2SO_4, $CHCl_3$, room temperature; (c) LiOH, THF, H_2O, room temperature; (d) **7**, DPTS, DIPC, CH_2Cl_2, room temperature; (e) H_2, Pd/C, MeOH, room temperature; (f) **12**, **10**, DPTS, DIPC, CH_2Cl_2, room temperature; (e) **13**, H_2, Pd/C, MeOH, room temperature.

and carbodiimide esterifications[16] (Scheme 2). The tertiary butyl[17] and benzyl groups[18] were selected because of their near quantitative cleavages (using trifluoroacetic acid or hydrogen chloride and hydrogen over Pd/C, respectively) and relative ease of introduction at multigram scales. The synthesis of compound **14** allows for the facile synthesis of DRCs with various rodcoils. The key factor in the synthesis of the conjugated segments **23**, **32**, and **39** is the coupling of the branched alkyl alcohol to the asymmetric aromatic handle through an ester or ether linkage prior to carbon−carbon bond formation (Schemes 3a, 4e, 5c). This linkage increases the solubility of the aromatic rod in the subsequent synthetic steps.[19,20] The branched alkane was selected as the coil segment because of its excellent solubility characteristics[13] and stability to all subsequent reaction conditions.

The synthesis of each conjugated rod segment in the DRC series studied here is accomplished using a different carbon−carbon bond forming reaction (Stille,[21,22] Horner−Emmons,[20,23]

(16) Moore, J. S.; Stupp, S. I. *Macromolecules* **1990**, *23*, 65−70.
(17) Alexakis, A.; Gardette, M.; Colin, S. *Tetrahedron Lett.* **1988**, *29*, 2951−2954.
(18) Denieul, M. P.; Laursen, B.; Hazell, R.; Skrydstrup, T. *J. Org. Chem.* **2000**, *65*, 6052−6060.
(19) Malenfant, P. R. L.; Jayaraman, M.; Frechet, J. M. J. *Chem. Mater.* **1999**, *11*, 3420−3422.
(20) Tew, G. N.; Pralle, M. U.; Stupp, S. I. *J. Am. Chem. Soc.* **1999**, *121*, 9852−9866.
(21) Scott, W. J.; Crisp, G. T.; Stille, J. K. *J. Am. Chem. Soc.* **1984**, *106*, 4630−4632.
(22) Facchetti, A.; Deng, Y.; Wang, A. C.; Koide, Y.; Sirringhaus, H.; Marks, T. J.; Friend, R. H. *Angew. Chem., Int. Ed.* **2000**, *39*, 4547−4551.
(23) Boutagy, J.; Thomas, R. *Chem. Rev.* **1974**, *74*, 87−99.

Scheme 3. Synthesis of Quaterthiophene Phenyl Rodcoil[a]

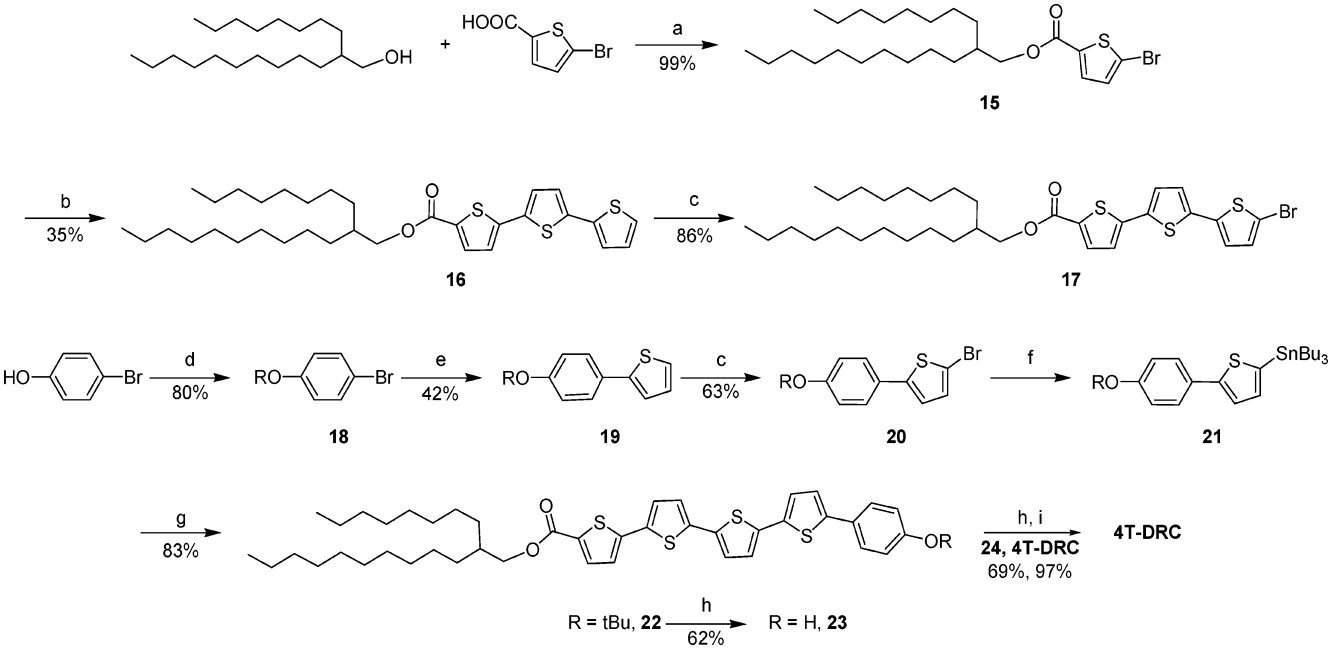

[a] (a) DIPC, DPTS, CH_2Cl_2, room temperature; (b) **15**, Bu_3Sn bithiophene, $Pd(PPh_3)_4$, DMF, 90 °C; (c) NBS, DMF, 0 °C to room temperature; (d) isobutylene, H_2SO_4, $CHCl_3$, room temperature; (e) Bu_3Sn thiophene, $Pd(PPh_3)_4$, DMF, 90 °C; (f) *n*BuLi, Bu_3SnCl, THF, −78 °C to room temperature; (g) **17**, **21**, $Pd(PPh_3)_4$, DMF, 110 °C; (h) TFA, CH_2Cl_2, room temperature; (i) **23**, **14**, DPTS, DIPC, CH_2Cl_2, room temperature; (j) TFA, CH_2Cl_2, room temperature.

Scheme 4. Synthesis of Terphenylene Vinylene Rodcoil[a]

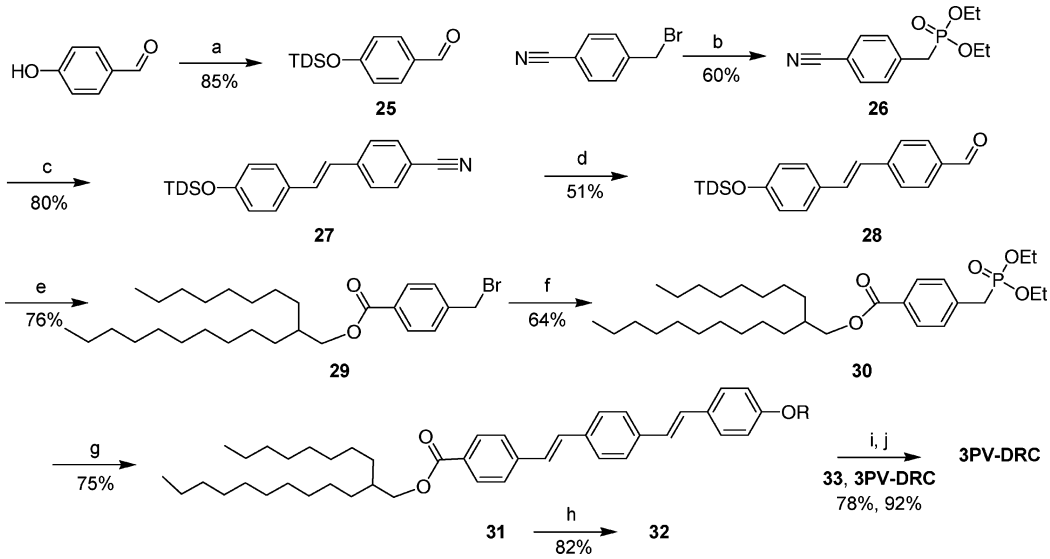

[a] (a) TDSCl, imidazole, CH_2Cl_2, room temperature; (b) triethyl phosphite, 130 °C; (c) **26**, LDA, **25**, THF, −78 °C to room temperature; (d) DIBALH, Et_2O, −78 to 0 °C; (e) 2-octyl-dodecan-1-ol and α-bromotoluic acid, DPTS, DIPC, CH_2Cl_2, room temperature; (f) triethyl phosphite, 130 °C; (g) **30**, LDA, **28**, THF, −78 °C to room temperature; (h) TBAF, THF, −78 °C; (i) **14**, **32**, DPTS, DIPC, CH_2Cl_2, room temperature; (j) HCl, dioxanes, room temperature.

and Suzuki[24,25] couplings). The synthesis of phenyl-quater-(thiophene) rodcoil (**23**) utilized Stille cross-coupling reactions. Bromination conditions (Scheme 3c) were adapted from the literature.[26] 4-Bromo phenol was utilized as an aromatic handle for facile incorporation of the thiophene rod into the ester-based DRC architecture due to tautomerization of 3-hydroxythiophenes.[27] The synthesis of the hydroxyphenyl quater(thiophene) rodcoil was convergent to avoid solubility problems (Scheme 3g). The synthesis of the ter(phenylene-vinylene) rodcoil (**32**) utilized Horner−Emmons couplings to form exclusively trans olefins in the phenylene vinylene rod.[20] Using lithium diisopropyl amide as a base at −78 °C in the Horner−Emmons couplings avoided ester and silyl ether cleavage (Scheme 4 c and g). The dimethylthexyl silyl protecting group was cleaved with tetrabutylammonium fluoride at −78 °C to avoid ester cleavage. Suzuki coupling 4′-bromo-[1,1′-biphenyl]-4-carboxylic acid was not readily available. The 4′-bromo-[1,1′-biphenyl]-4-ol was reacted with the branched alkyl mesylate under standard

(24) Watanabe, T.; Miyaura, N.; Suzuki, A. *Synlett* **1992**, 207−210.
(25) Ohe, T.; Miyaura, N.; Suzuki, A. *J. Org. Chem.* **1993**, *58*, 2201−2208.
(26) Bauerle, P.; Wurthner, F.; Gotz, G.; Effenberger, F. *Synthesis* **1993**, 1099−1103.
(27) Capon, B.; Kwok, F.-C. *Tetrahedron Lett.* **1986**, *27*, 3275−3278.

Scheme 5. Synthesis of Quaterphenylene Rodcoil[a]

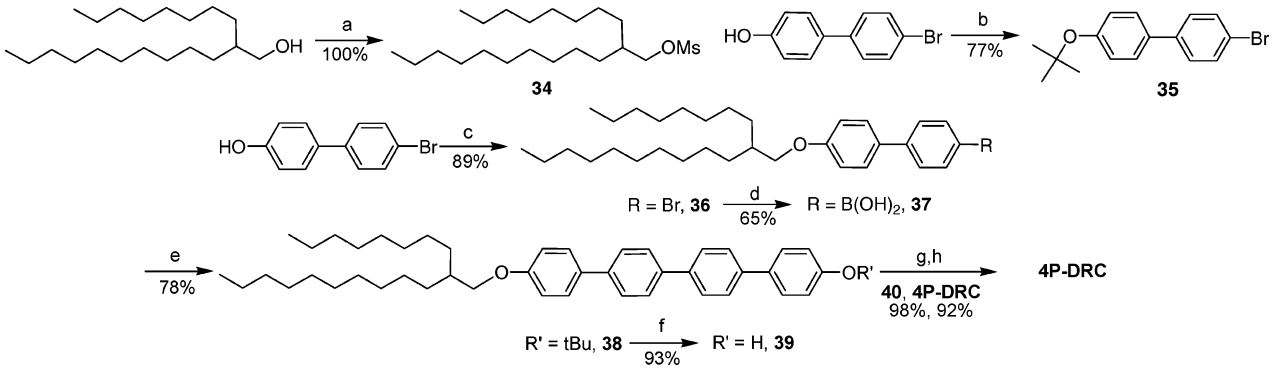

[a] (a) MsCl, TEA, CH_2Cl_2, room temperature; (b) isobutylene, H_2SO_4, $CHCl_3$, room temperature; (c) **34**, K_2CO_3, 18-crown-6, acetone, reflux; (d) *n*BuLi, $B(OMe)_3$, HCl; (e) **37**, **35**, $Pd(PPh_3)_4$, Na_2CO_3, toluene, EtOH, H_2O, reflux; (f) TFA, CH_2Cl_2, room temperature; (g) **14**, DPTS, DIPC, CH_2Cl_2, room temperature; (h) TFA, CH_2Cl_2.

conditions[28] (Scheme 5c), and the boronic acid[29] was synthesized from the solubilized 4-bromo-4′-alkyloxy-biphenyl (Scheme 5d). The 4′-bromo-[1,1′-biphenyl]-4-ol was tertiary butyl protected using isobutylene and catalytic H_2SO_4 and was reacted under Suzuki conditions with the boronic acid.

Self-Assembly. Our initial attempts at designing the conjugated DRC series involved the complete replacement of the three biphenyl-ester units of the original DRC molecule[13] for a shorter conjugated segment. For example, we synthesized molecules **4** and **6** in Scheme 1. These molecules can be dissolved at high temperatures in toluene. Upon cooling, however, we observed precipitation rather than gelation, suggesting that extensive one-dimensional self-assembly does not occur. Molecule **5** does exhibit gelation without the added length of a biphenyl segment, pointing out how subtle are the required noncovalent interactions between rod segments to trigger the assembly of high aspect ratio nanostructures. As prepared in tetrahydrofuran (THF), DRC samples absorb and fluoresce at wavelengths corresponding to the fully solvated chromophores[30] (Figure 1a, Table 1). At the same concentration, 30:1 toluene:THF, **4T-DRC**, **3PV-DRC**, and **4P-DRC** form self-supporting, birefringent gels after dissolution by heating to 110 °C and subsequent cooling to room temperature (Figure 1b). The self-assembly behaviors of **4T-DRC**, **3PV-DRC**, and **4P-DRC** are remarkably similar despite their structural variations. The added length of the biphenyl segment increases the ability of rod segments to $\pi-\pi$ stack, but also adds additional rotational degrees of freedom about the ester bond.

The formation of a gel at low concentrations (1 wt %) suggests self-assembly of DRC molecules into high aspect ratio nanostructures.[11,13,31,32] Upon gelation of the DRC series, absorbance is blue-shifted and fluorescence emission red-shifts. The shifts in absorbance and fluorescence maxima are consistent with exciton coupling of the aromatic units due to the formation of H aggregates.[33] The absorption and fluorescence intensity of the DRCs decreases in the assembled state, typical of other aggregated systems due to increased scattering as well as fluorescence quenching in the aggregated state[10,34,35] (Figure 1, Table 1, Supporting Information). Solution NMR reveals further evidence of DRC aggregation. The aromatic peaks of **4T-DRC** in THF-d_8 are unresolved in toluene-d_8 (Figure 2). The aliphatic protons, however, persist in toluene-d_8, broadening only slightly. This indicates more rotational freedom of the alkyl coil segment relative to the aromatic rod-like segment.[13,36]

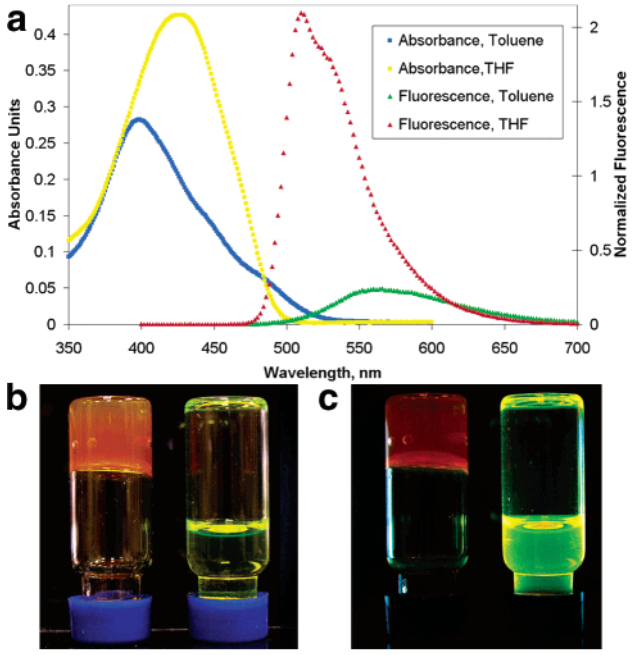

Figure 1. (a) Absorbance and fluorescence emission spectra of **4T-DRC** gel dissolved in toluene and THF. (b) White light illuminated photographs of **4T-DRC** in toluene (left) and THF (right). (c) 365 nm light illuminated photographs of **4T-DRC** in toluene (left) and THF (right).

Table 1. Optical Behavior of DRCs

	λ_{max} (nm)[a]		λ_{max} (nm)[b]	
	toluene	THF	toluene	THF
4T-DRC	398	424	566	510
3PV-DRC	337	367	444	473
4P-DRC	296	305	424	418

[a] Absorption. [b] Emission.

(28) Claussen, R. C.; Rabatic, B. M.; Stupp, S. I. *J. Am. Chem. Soc.* **2003**, *125*, 12680−12681.
(29) Liess, P.; Hensel, V.; Schluter, A. D. *Liebigs Ann.* **1996**, 1037−1040.
(30) Wei, Y.; Yang, Y.; Yeh, J. M. *Chem. Mater.* **1996**, *8*, 2659−2666.
(31) Terech, P.; Weiss, R. G. *Chem. Rev.* **1997**, *97*, 3133−3159.
(32) Hartgerink, J. D.; Beniash, E.; Stupp, S. I. *Science* **2001**, *294*, 1684−1688.
(33) Kasha, M.; Rawls, H. R.; El-Bayoumi, M. A. *Pure Appl. Chem.* **1965**, *11*, 371−392.
(34) Schenning, A.; Jonkheijm, P.; Peeters, E.; Meijer, E. W. *J. Am. Chem. Soc.* **2001**, *123*, 409−416.
(35) Whitten, D. G. *Acc. Chem. Res.* **1993**, *26*, 502−509.

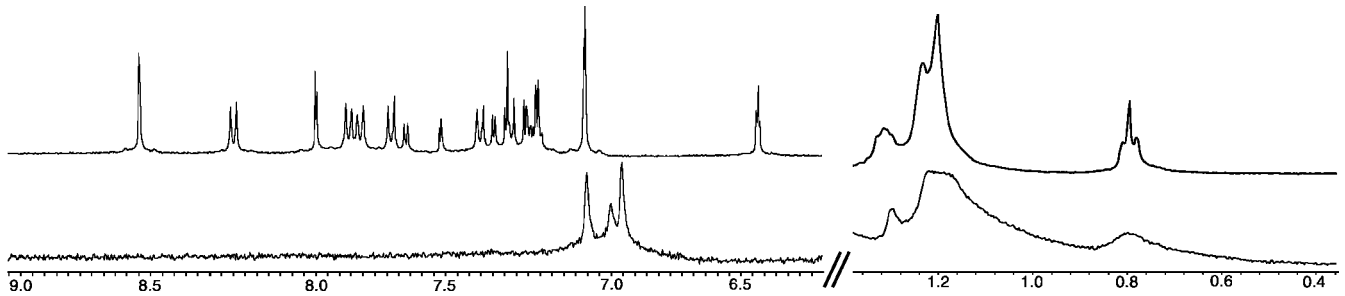

Figure 2. NMR of **4T-DRC** in THF-d_8 (top) and in toluene-d_8 (bottom) (the signals in the toluene spectrum at 7 ppm are residual solvent peaks from toluene-d_8).

Table 2. Small-Angle X-ray Diffraction Peaks Taken from Dried Films of DRC Gels (±0.2 nm)[a]

molecule	spacing (nm)
4T-DRC	10.0
3PV-DRC	10.3
4P-DRC	9.1

[a] Peaks were fit after integration of the 2D diffraction pattern and background subtraction using a standard Gaussian−Lorentzian curve-fitting algorithm.

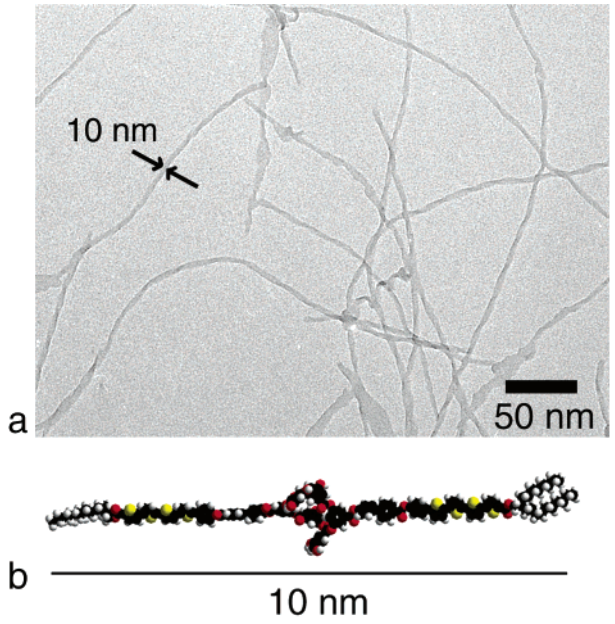

Figure 3. (a) TEM micrograph of **4T-DRC** ribbons cast on amorphous carbon. (b) Molecular graphics of two DRC molecules measuring to be 10 nm.

X-ray scattering and microscopy of the series reveals the self-assembly of DRC molecules into ribbon-like nanostructures. Small-angle X-ray scattering (SAXS) spectra of dried DRC gels contain diffraction peaks with characteristic *d* spacings due to the solid-state packing of the ribbon structures, as summarized in Table 2. The major peak matches the ribbon width observed in transmission electron microscopy (TEM) (Figure 3a) and is consistent with the fully extended length of two molecules, as determined from molecular graphics (Figure 3b). While the exact nature of the dendron interaction is unclear, hydrogen bonding in the hydroxyl-rich dendron appears to play a significant role.[13] For TEM observations, a dilute solution of nanostructures of **4T-DRC** was cast from toluene and dried onto a holey carbon coated grid. While TEM revealed several different morphologies for the self-assembled structure of **4T-DRC**, the dominant one observed was a twisted, high aspect ratio nanostructure with a remarkably uniform diameter of 9.3 ± 0.7 nm. The atomic force microscopy (AFM) images of similarly prepared samples on a freshly cleaved mica surface show ribbon-like features with thicknesses of 2−6 nm. Figure 4 shows AFM images of the ribbon nanostructures of **3PV-DRC** and **4P-DRC**.

We conclude that DRC molecules dissolved in toluene self-assemble into ribbon-like nanostructrues. Self-assembly is evident macroscopically by changes in solvent flow (the formation of a self-supporting gel) due to an interconnected network of one-dimensional nanostructures. The nanostructures have ribbon morphologies with $\pi-\pi$ stacked conjugated segments as evidenced by X-ray, TEM, AFM, optical, and NMR spectroscopies. These one-dimensional scaffolds formed by DRC molecules offer a strategy to create ordered arrays of electronically active molecules.

Conductivity and Alignment of 4T-DRC. As described above, DRC self-assembly directly affects the physical behavior of these materials. In addition, we explored the effect of self-assembly on the electronic properties of solid-state films cast from gels of **4T-DRC** nanostructures. Casting from an assembled state results in a film of supramolecular nanostructures instead of the amorphous or crystalline films expected when casting films from oligo(thiophene) solutions.[4] Iodine-doped films of **4T-DRC** were prepared from 1 wt % gels (assembled) and THF solutions (solvated) of **4T-DRC**. The films cast from the self-assembled state were strongly birefringent, and preparation on a patterned, four-probe electrode (Figure 5) indicated conductivities of 7.9×10^{-5} S/cm. In great contrast, films cast from THF solutions in which self-assembly does not occur exhibit conductivities that are 3 orders of magnitude lower (8.0×10^{-8} S/cm, p-value < 0.01). In our model of 4T-DRC assembly outlined above, $\pi-\pi$ stacking plays a major role. We believe the 3 orders of magnitude increase in conductivity is most likely due to improved π-orbital overlap along conductive pathways in the ribbon-like nanostructures. It is possible that a similar enhancement could be observed due to conformational or packing effects in the thiophene segments. In either case, however, the increase in conductivity is clearly a result of self-assembly.

Alignment of nanoribbons can be accomplished by solution casting films in an alternating current (AC) electric field. In an AC field, the nanostructures become charged and oscillate due to electrophoresis. Shear forces align the nanoribbons parallel to the electric field lines, resulting in a uniaxially aligned film

(36) Ahrens, M. J.; Sinks, L. E.; Rybtchinski, B.; Liu, W.; Jones, B. A.; Giaimo, J. M.; Gusev, A. V.; Goshe, A. J.; Tiede, D. M.; Wasielewski, M. R. *J. Am. Chem. Soc.* **2004**, *126*, 8284−8294.

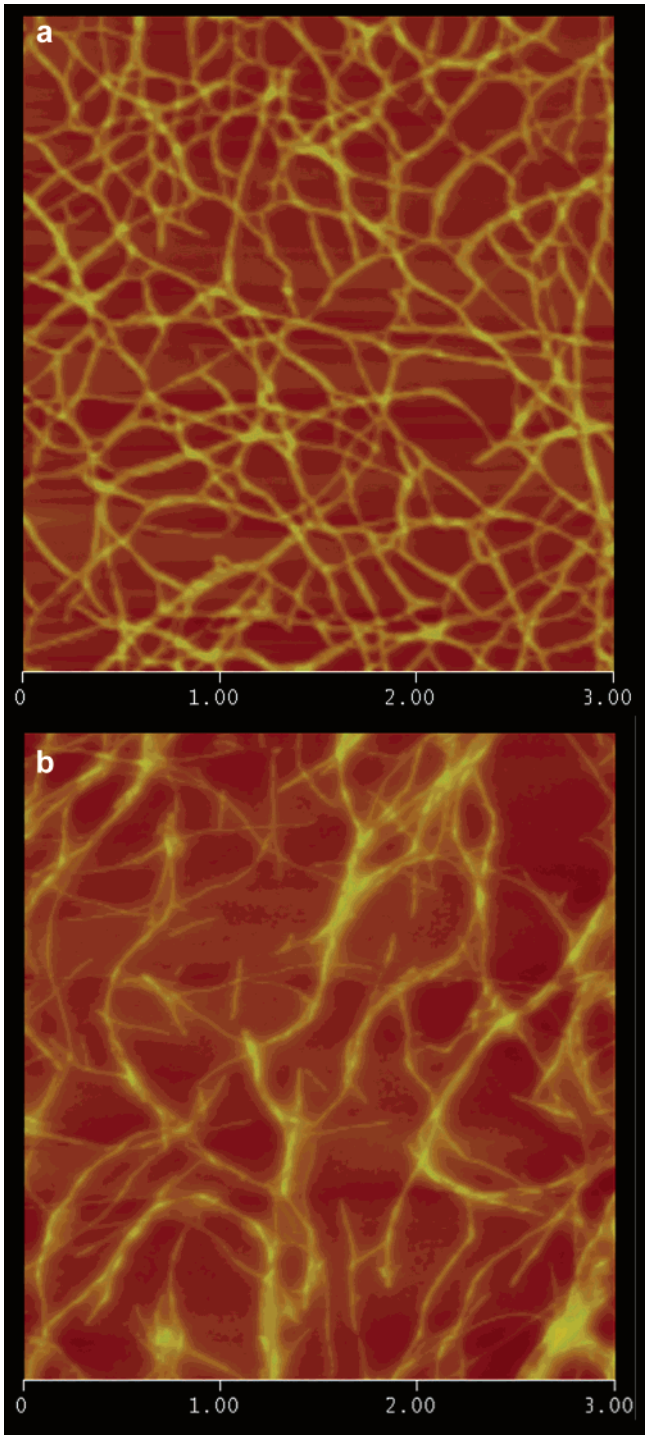

Figure 4. AFM images of **3PV-DRC** (a) and **4P-DRC** (b) on mica (scalebar in micrometers).

of ribbon nanostructures, similar to other one-dimensional systems.[37,38] When viewed by polarized optical microscopy, the birefringent film switches from light to dark upon a 45° rotation between crossed polarizers (Figure 6a and b, respectively). Ribbon alignment was also observed directly with AFM, using a dilute gel on mica aligned between two electrodes by an AC field. Ribbons in the gap show alignment parallel to the electric field (Figure 7). According to the model of assembly, the $\pi-\pi$ stacking direction and the long axis of the ribbon nanostructures are parallel to each other.

(37) Krupke, R.; Hennrich, F.; von Lohneysen, H.; Kappes, M. M. *Science* **2003**, *301*, 344−347.
(38) Thurn-Albrecht, T.; DeRouchey, J.; Russell, T. P.; Kolb, R. *Macromolecules* **2002**, *35*, 8106−8110.

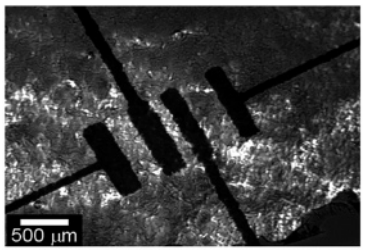

Figure 5. Polarized optical micrograph showing birefringent **4T-DRC** film cast from a toluene gel on a four-point probe electrode structure.

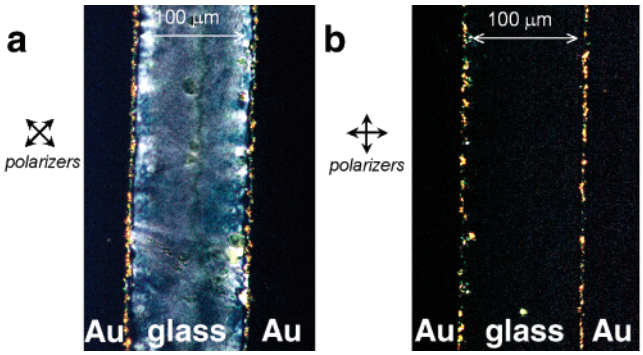

Figure 6. Polarized optical microscopy of an AC field aligned **4T-DRC** film. The film switches from light (a) to dark (b) with a 45° rotation between crossed polarizers, indicating uniaxial orientation of the optic axis of the film.

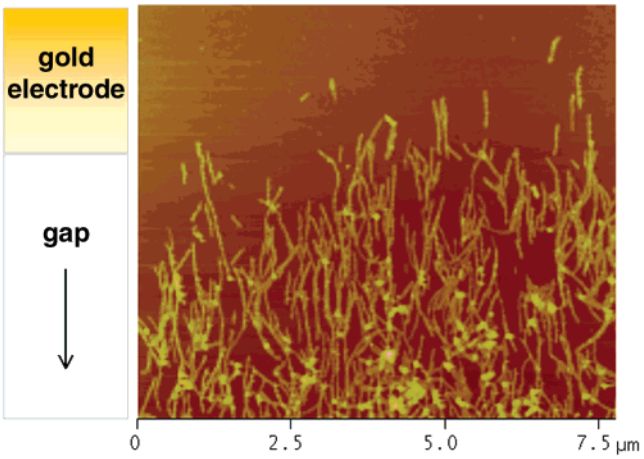

Figure 7. Atomic force microscopy image of aligned ribbons of **4T-DRC** on Au/Cr patterned mica substrate. The diagram (left) depicts where the edge of the gold electrode begins on the substrate. Ribbons are aligned in the gap.

Conclusions

The dendron rodcoil molecular architecture is a unique and versatile structure to program the self-assembly of high aspect ratio supramolecular polymers. We have shown that various conjugated structures can be incorporated into dendron rod coils without disrupting their one-dimensional self-assembly. The self-assembly of the conjugated molecules into supramolecular ribbon nanostructures leads to enhanced electronic conductivity due to improved π-orbital overlap. Furthermore, these supramolecular polymers can be oriented macroscopically in external fields, which might be useful in bottom-up device fabrication.

Acknowledgment. This work made use of the Keck Biophysics Facility, the NIFTI Center, EPIC, and the Analytical Services Laboratory at Northwestern University. B.W.M. would like to thank Prof. E. Zubarev for helpful discussions, Prof. M. Hersam, and M. Arnold for assistance with conductivity measurements and S. Bull for MS measurements. The work was supported by the U.S. Department of Energy (DoE) under Award No. DE-FG02-00ER54810 and the Air Force Office of Scientific Research (AFOSR) Multidiciplinary University Research Initiative (MURI) under award number F49620-00-1-0283.

Supporting Information Available: Synthetic information, additional UV−vis and fluorescence spectra, SAXS 2D integrations, and AFM. This material is available free of charge via the Internet at http://pubs.acs.org.

JA049325W